

Title	Theoretical Consideration on Nonlinear Compensation Method for Minimizing High Order Intermodulation Distortion Nonlinear Compensation in a Direct Optical FM RoF System
Author(s)	Murakoshi, Akihiko; Tsukamoto, Katsutoshi; Komaki, Shozo
Citation	IEICE Transactions on Electronics. 2003, E86-C(7), p. 1167-1174
Version Type	VoR
URL	<a href="https://hdl.handle.net/11094/3431">https://hdl.handle.net/11094/3431</a>
rights	copyright©2008 IEICE
Note	

***Osaka University Knowledge Archive : OUKA***

<https://ir.library.osaka-u.ac.jp/>

Osaka University

# Theoretical Consideration of Nonlinear Compensation Method for Minimizing High-Order Intermodulation Distortion Nonlinear Compensation in a Direct Optical FM RoF System

Akihiko MURAKOSHI<sup>†a)</sup>, Student Member, Katsutoshi TSUKAMOTO<sup>†</sup>, Regular Member, and Shozo KOMAKI<sup>†</sup>, Fellow

**SUMMARY** An optical FM system using an optical FM LD (laser diode) and an optical frequency discriminator (OFD), in which a nonlinear compensation scheme based on the interaction between its nonlinearities can minimize intermodulation distortion. This paper theoretically investigates the minimization influence for 3rd plus 5th order intermodulation distortion power for an optical FM radio-on-fiber system. The carrier to noise-plus-distortion power ratio (CNDP) is theoretically analyzed in employing the OFD whose transmission characteristic is controlled by a phase shifter. The results show that the designed receiver can achieve higher CNDP in the application of multicarrier transmission.

**key words:** radio-on-fiber (RoF), optical FM, optical frequency discriminator (OFD), intermodulation distortion

## 1. Introduction

When employing a conventional optical intensity modulation/direct detection (IM/DD) scheme in a radio-on-fiber (RoF) link [1]–[4] to transmit multicarrier RF signals containing CATV, wireless LAN signals and so on, the RF signal quality is severely degraded by intermodulation distortion and clipping distortion when modulating the LD [5], [6].

As a candidate to solve the above problems, frequency modulations methods have been investigated, such as a SCM (subcarrier multiplexing)/FM/IM/DD method for obtaining a wideband gain [7], [8] and Optical FM method which is effective in clipping distortion [9]–[16]. The combined effect of LD and OFD nonlinearities except for signal quality such as CDR have been reported [12], [13]. In references [14]–[16] a nonlinear distortion compensation method for a RoF link by using an interaction between the nonlinearities of an optical LD and MZI-type OFD is proposed, and it has its transmission performance analyzed and the carrier to noise-plus-distortion power ratio (CNDP) calculated theoretically. These previous studies have considered

only 3rd-order intermodulation (IM3) distortion power in a single-octave transmissions and designed a receiver to minimize the IM3 distortion power [14]–[16]. However if a large number of frequency channels like OFDM signals or multioctave multicarrier signals are applied, intermodulation distortion powers including 5th (IM5) order or higher order distortion, should be considered in RF signal transmission.

In this study, we investigate the optical FM method using a LD and a MZI-type OFD in SCM RF signal transmission and design a receiver that minimizes intermodulation distortion power by using a phase shifter. Then we focus on the theoretical analysis of IM3 and IM5 distortion power, the phase shift,  $\phi$ , that minimizes IM3 plus IM5 distortion power, and CNDP including IM3 and IM5 distortion in the system using an optical FM method. Finally, we show that CNDP in using the designed receiver is more improved than CNDP in controlling the phase shift which minimizes IM3 distortion power and IM3 plus IM5 distortion power and without phase shifter control.

This paper is organized as follows. In Sect. 2, we describe the configuration of the RoF link using an optical FM LD and a MZI-type OFD and mathematically models their nonlinearity and the characteristic of the MZI-type OFD with a phase shifter. In Sect. 3 we theoretically analyze IM3 plus IM5 distortion power, and the phase shift that minimizes IM3 plus IM5 distortion power in this system. Finally, in Sect. 4, we show the availability of phase shifter control for IM3 plus IM5 distortion power numerically.

## 2. Nonlinear Compensation Scheme in SCM FM RoF Link

Figure 1 shows the configuration of the SCM RoF link using a nonlinear compensation scheme. A SCM RF signal is received at a radio base station (RBS) and modulates the frequency of the LD. The modulation frequency of the LD is given by [16]

$$f(t) - f_c = f_m(t) = \alpha i_{in}(t) + \beta i_{in}^2(t) + \gamma i_{in}^3(t) \quad (1)$$

Manuscript received December 2, 2002.

Manuscript revised February 10, 2003.

<sup>†</sup>The authors are with the Department of Communications Engineering, Graduate School of Engineering, Osaka University, Suita-shi, 565-0871 Japan.

a) E-mail: murakosi@roms.comm.eng.osaka-u.ac.jp

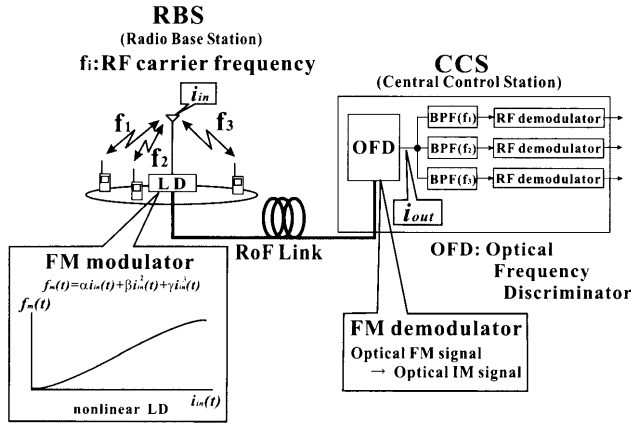


Fig. 1 Configuration of RoF link using direct optical FM and OFD.

where  $f(t)$  is the Optical FM signal frequency,  $f_c$  is an optical carrier frequency, that is a driving point,  $\alpha$  is the modulation efficiency,  $\beta$  and  $\gamma$  are coefficients of the 2nd and 3rd distortion, and  $i_{in}(t)$  is the SCM RF signal current [15]. After transmission via optical fiber, the optical FM signal is converted into an optical IM signal at the MZI-type OFD whose transmissions  $T_1(f)$  and  $T_2(f)$  shown in Fig. 2(a) [15] are given by

$$T_l(f) = \frac{1}{2} \left[ 1 \mp \cos \left( \frac{\pi f}{FSR} \right) \right] \quad (l = 1, 2), \quad (2)$$

where FSR denotes the free spectral range of MZI. Here, the transmission characteristic of the MZI-type OFD is expanded in the Taylor series as

$$T_l(f) = \sum_{j=0}^{\infty} \frac{1}{j!} T_l^{(j)} \{f_m(t)\}^j \quad (l = 1, 2), \quad (3)$$

where  $T_l^{(j)}$  is given by

$$T_l^{(j)} = \frac{d^j}{df^j} T_l(f) \Big|_{f=f_c} = \begin{cases} \frac{1}{2} \mp \frac{1}{2} \cos \left( \frac{\pi f_c}{FSR} \right) & (j = 0) \\ \mp \frac{1}{2} \left( \frac{\pi}{FSR} \right)^j \cos \left( \frac{\pi f_c}{FSR} + \frac{j\pi}{2} \right) & (j = 1, 2, \dots) \end{cases} \quad (l = 1, 2). \quad (4)$$

On the other hand, the transmission characteristic of the MZI-type OFD with the phase shifter shown in Fig. 2(b) is expressed by [16]

$$T_l(f, \phi) = \frac{1}{2} \left[ 1 \mp \cos \left( \frac{\pi f}{FSR} + \phi \right) \right] \quad (l = 1, 2), \quad (5)$$

where  $\phi$  is the phase shift at the phase shifter. Similarly  $T_l(f, \phi)$  is expressed in the Taylor series [16] by

$$T_l(f, \phi) = \sum_{j=0}^{\infty} \frac{1}{j!} T_l^{(j)}(\phi) \{f_m(t)\}^j \quad (6)$$

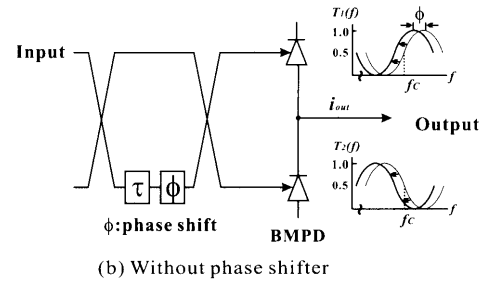
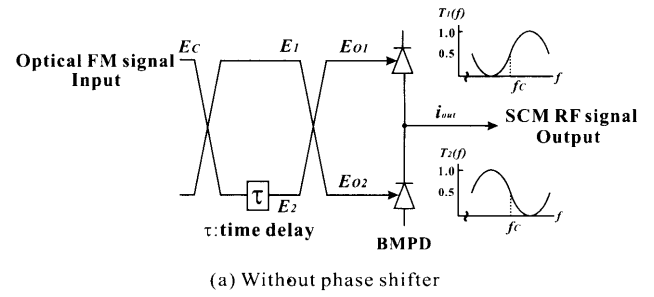


Fig. 2 MZI type OFD.

$$T_l^{(j)}(\phi) = \begin{cases} \frac{1}{2} \mp \frac{1}{2} \cos \left( \frac{\pi f_c}{FSR} + \phi \right) & (j = 0) \\ \mp \frac{1}{2} \left( \frac{\pi}{FSR} \right)^j \cos \left( \frac{\pi f_c}{FSR} + \frac{j\pi}{2} + \phi \right) & (j = 1, 2, \dots) \end{cases} \quad (l = 1, 2). \quad (7)$$

It is found from Eq. (7) that the transmission characteristic of the MZI-type OFD can be shifted using a phase shifter.

From Eqs. (1) and (5)–(7) the photodetector output current,  $i_{out}(t)$ , is

$$i_{out}(t) = rP_c \left[ 1 + \frac{\alpha}{\Delta F} m_k i_{in}(t) \right] \{T_1(f, \phi) - T_2(f, \phi)\} + n(t) = -rP_c \left[ 1 + \frac{\alpha}{\Delta F} m_k i_{in}(t) \right] \sum_{j=0}^{\infty} \frac{1}{j!} T_1^{(j)}(\phi) \{f_m(t)\}^j + n(t), \quad (8)$$

where  $r$ ,  $P_c$ ,  $\Delta F$ ,  $n(t)$ ,  $f_c$ , and  $m_k$  are the sensitivity of PD, the received optical power, the maximum frequency deviation, the additive noise current, the optical carrier frequency, and the intensity modulation index, respectively.

We substitute Eq. (1) into Eq. (8) and calculate the components of the signal and intermodulation distortions. The carrier power,  $C$ , IM3 distortion power,  $D_3$ , and IM5 distortion power,  $D_5$ , falling in the  $n$ th frequency channel,  $f_n$ , of the received RF signal are derived by

$$C = \left[ 2T_1(\phi)^{(1)} \alpha r P_c \right]^2 \langle (i_{in}(t))^2 \rangle_{f_n} \quad (9)$$

$$D_3 = \left[ 2rP_c \left\{ \gamma T_1^{(1)}(\phi) + \alpha \beta T_1^{(2)}(\phi) + \frac{\alpha^3}{3!} T_1^{(3)}(\phi) \right\} \right]^2 \langle (i_{in}(t))^3 \rangle_{f_n}$$

$$+ \frac{\alpha m_k}{\Delta F} \left( \beta T_1^{(1)}(\phi) + \alpha^2 T_1^{(2)}(\phi) \right) \left\langle (i_{in}^3(t))^2 \right\rangle_{f_n} \quad (10)$$

$$D_5 = \left[ 2rP_c \left\{ \beta \gamma T_1^{(2)}(\phi) + \frac{1}{3!} (\alpha^2 \gamma + 3\alpha \beta^2) T_1^{(3)}(\phi) \right. \right. \\ \left. \left. + \frac{3}{4!} \alpha^3 \beta T_1^{(4)}(\phi) + \frac{\alpha^5}{5!} T_1^{(5)}(\phi) \right. \right. \\ \left. \left. + \frac{\alpha m_k}{\Delta F} \left( (2\alpha \gamma + \beta^2) T_1^{(2)}(\phi) + 3\alpha^2 \beta T_1^{(3)}(\phi) \right. \right. \right. \\ \left. \left. \left. + \alpha^4 T_1^{(4)}(\phi) \right) \right\} \right]^2 \left\langle (i_{in}^5(t))^2 \right\rangle_{f_n}, \quad (11)$$

where  $\langle \bullet \rangle$  is the ensemble average.

We explain the physical mechanism of IM3 and IM5 generations. Figures 3 and 4 illustrate the mechanism of IM3 and IM5 generation in this system. The first term in  $\{*\}$  of IM3 shown in Eq. (10) is composed of the 3rd-order nonlinearity of the LD. The second term is composed of the multiplication of the linearity, and the 2nd order nonlinearity of the LD for the 2nd nonlinearity of OFD. The third term is composed of the cube of the signal for the 3rd-order nonlinearity of the OFD. The last term is composed of the multiplication of the intensity modulation component and the 2nd-order intermodulation distortions. Moreover, the first term in  $\{*\}$  of IM5 shown in Eq. (11) is composed of the multiplication of the 2nd- and 3rd-order nonlinearities, for the 2nd order nonlinearity of the OFD. The second term is composed of the multiplication of the linearity, and the 3rd-order nonlinearity of the LD

for the 3rd-order nonlinearity of the OFD. The third and fourth terms are composed of the multiplication of the linearity, and the 2nd orders-nonlinearity of the LD for the 4th-order nonlinearity of the OFD, and the 5th-order of linearity for the 5th-order nonlinearity of the OFD, respectively. The last term is composed of the multiplication of the intensity component and the 4th-order intermodulation distortions. Figures 3 and 4 also illustrate the above explanation.

In the case of IM3, it is found from Eq. (7) that  $T_1^{(1)}(\phi)$  and  $T_1^{(3)}(\phi)$  have anti-sign each other. Consequently the phase shift  $\phi$  which minimizes  $D_3$  can be found regardless of the sign of  $T_1^{(2)}(\phi)$  and IM3 distortion power can be reduced. For IM5, a similar reduction can be obtained. Therefore, we can expect that the nonlinearity component of the OFD at the receiver has the potential ability to reduce IM3 or IM5.

The noise power,  $N$ , is given by [15]

$$N = \left\{ 2qrP_c + \frac{4kT}{R_t} + \frac{\Delta\nu}{\pi} \left( rP_c T_1^{(1)}(\phi) \right) \right\} B \\ + \frac{1}{2} \left\{ m_k \left( T_1^{(0)}(\phi) - T_2^{(0)}(\phi) \right) \right\}^2, \quad (12)$$

where  $q$  is an electrical charge,  $B$  is the bandwidth of BPF at the RF stage,  $k$  is the Boltzmann constant,  $T$  is the equivalent noise temperature,  $R_t$  is the equivalent noise resistance and  $\Delta\nu$  is the full width at half maximum of the optical carrier spectrum. The first term, second term, third term, and last term in Eq. (12) are the shot noise power, the thermal noise power in the receiver, the phase noise power, and the optical intensity noise power, respectively.

### 3. IM3 and IM5 Distortion Power with Nonlinear Compensation in SCM FM RoF Link

In order to analyze IM3 and IM5 distortion power theoretically, we assume a SCM RF current,  $i_{in}(t)$ , with  $2K + 1$  channels given by

$$i_{in}(t) = \sum_{n=-K}^K R_n(t) \cos \{ 2\pi (f_{RF} + n\delta f) t + \psi_n(t) \}, \quad (13)$$

where  $n$ ,  $f_{RF}$ ,  $\delta f$ ,  $R_n(t)$ , and  $\psi_n(t)$  are the integer, the central RF frequency of the channel, the channel spacing, the envelope of the  $n$ th channel, and the phase of the  $n$ th channel which is a random variable, respectively. And  $n$ th channel,  $f_n$ , is expressed as

$$f_n = f_{RF} + n\delta f \\ R_n(t) = R(\text{const}) \quad \text{for all } n$$

At the output RF current shown in Fig. 1,  $i_{in}^3(t)$ , and  $i_{in}^5(t)$  in Eqs. (10) and (11) are given by

$$i_{in}^3(t) = \sum_{n=-K}^K \frac{A_{3n}}{4} R^3 \cos 2\pi (f_{RF} + n\delta f) t \quad (14)$$

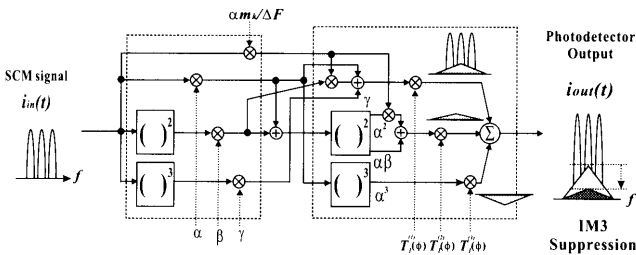


Fig. 3 Mechanism of IM3 generation in optical FM and OFD RoF system.

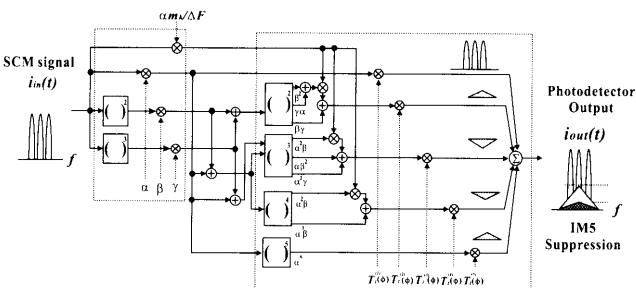


Fig. 4 Mechanism of IM5 generation in optical FM and OFD RoF system.

$$i_{in}^5(t) = \sum_{n=-K}^K \frac{A_{5n}}{16} R^5 \cos 2\pi (f_{RF} + n\delta f) t. \quad (15)$$

The relationship among  $\Delta F$ ,  $\alpha$  and  $R$  is expressed as

$$\Delta F = \alpha R \quad (16)$$

Consequently  $\langle (i_{in}^3(t))^2 \rangle_{f_n}$  and  $\langle (i_{in}^5(t))^2 \rangle_{f_n}$  in Eqs. (10) and (11) are derived as

$$\langle (i_{in}^3(t))^2 \rangle_{f_{RF}+n\delta f} = \frac{1}{2} \left( \frac{A_{3n}}{4} \right)^2 \left( \frac{\Delta F}{\alpha} \right)^6 \quad (17)$$

$$\langle (i_{in}^5(t))^2 \rangle_{f_{RF}+n\delta f} = \frac{1}{2} \left( \frac{A_{5n}}{16} \right)^2 \left( \frac{\Delta F}{\alpha} \right)^{10}, \quad (18)$$

where  $A_{3n}$  and  $A_{5n}$  are the number of IM3 and IM5 components falling in  $f_{RF} + n\delta f$  frequency channel, respectively.

It is found from Eqs. (17) and (18) that  $D_3$  and  $D_5$  increase in proportion to the 6th and 10th powers of the maximum frequency deviation,  $\Delta F$ , respectively. Therefore the influence of IM5 distortion power is not negligible if the number of the carrier,  $2K+1$ , and the maximum frequency deviation,  $\Delta F$ , become large. In Sect. 4, we discuss the influence of IM5 distortion.

$D_3$  and  $D_5$  have a maximum value at 0th channel, that is at the  $f_{RF}$  channel. We focus on the evaluation of the  $f_{RF}$  channel. From Eq. (10), the phase shift when  $D_3$  becomes zero can be solved and is given by (see Eq. (A.5))

$$\phi_{D3} \triangleq n\pi - \frac{\pi f_c}{FSR} - \theta_3, \quad n : \text{integer} \quad (19)$$

Similarly  $D_5 = 0$  from Eq. (11) when (see Eq. (A.6))

$$\phi_{D5} \triangleq n\pi - \frac{\pi f_c}{FSR} - \theta_5, \quad n : \text{integer} \quad (20)$$

where  $\theta_3$  and  $\theta_5$  are given by

$$\theta_3 = \tan^{-1} \left[ \frac{\frac{\pi}{FSR} (\alpha\beta + \frac{1}{2} \frac{m_k}{\Delta F} \alpha^3)}{\gamma + \frac{m_k}{\Delta F} \alpha\beta - \frac{1}{6} \left( \frac{\pi}{FSR} \right)^2 \alpha^3} \right] \quad (21)$$

$$\theta_5 = \tan^{-1} \left\{ \beta\gamma - \frac{1}{8} \left( \frac{\pi}{FSR} \right)^2 \alpha^3 \beta + \frac{1}{2} (2\gamma\alpha + \beta^2) \frac{\alpha m_k}{\Delta F} - \frac{1}{24} \left( \frac{\pi}{FSR} \right)^2 \frac{m_k \alpha^5}{\Delta F} \right\} \\ \div \left\{ \frac{\pi}{FSR} \left( \frac{\alpha^5}{120} \left( \frac{\pi}{FSR} \right)^2 - \frac{1}{2} (\alpha\beta^2 + \alpha^2\gamma) - \frac{1}{2} \alpha^3 \beta \frac{m_k}{\Delta F} \right) \right\} \quad (22)$$

We find that from Eqs. (19) and (20)  $\phi_{D3}$  is not generally equal to  $\phi_{D5}$ .

Then we consider the phase shift which minimizes the total power of IM3 and IM5 distortions. Next

we consider the phase shift which minimizes the combination power of IM3 and IM5 distortions. We assume that the correlation between IM3 and IM5 become negligibly small. Then we examine the total distortion given by  $D_3 + D_5$ . Therefore we attempt to theoretically find a phase shift  $\phi_{min}$  to minimize  $D_3(\phi) + D_5(\phi)$  ( $\triangleq IMD(\phi)$ ).  $IMD(\phi)$  has the minimum value when (see Eq. (A.12) in Appendix)

$$\phi_{min} = n\pi - \frac{\pi f_c}{FSR} - \frac{1}{2} \tan^{-1} \frac{D_{IM3} \sin 2\theta_3 + D_{IM5} \sin 2\theta_5}{D_{IM3} \cos 2\theta_3 + D_{IM5} \cos 2\theta_5}. \quad (23)$$

Figure 5 illustrates the receiver with the phase shifter [15] and [16]. We assume that the intermodulation distortion powers contained in the nonsignal band of output SCM RF current can be detected at the power detector, and the phase shifter is controlled by the feedback circuit in order to minimize the detected intermodulation distortion power.

That is, the receiver controls its transmission characteristic in Eq. (6) to minimize intermodulation distortion power  $IMD(\phi)$ . A similar method for detection of distortion power has been studied [17].

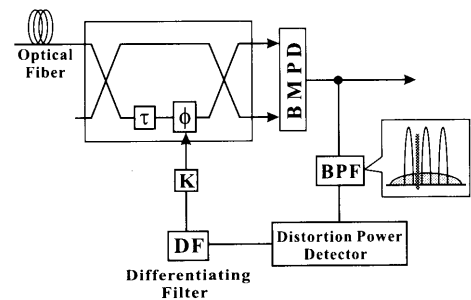


Fig. 5 The receiver with phase shifter.

Table 1 Parameters used in calculation.

FSR GHz	17.5	$P_c$ dBm	-10
$m_k$	0.01	$\Delta\nu$ MHz	0.5
$T$ K	300	$B$ KHz	300
$r$ A/W	0.8	$R_t$ $\Omega$	50

Table 2 Characteristic of LDs.

	nonlinear LD	linear LD
$\alpha$ MHz/mA	72	72
$\beta$ MHz/mA <sup>2</sup>	0.01	0
$\gamma$ MHz/mA <sup>3</sup>	0.001	0

Table 3 Some numerical results of  $D_7/D_3$  dB and  $D_7/D_5$  dB.

$\Delta F$ MHz	$D_7/D_3$ dB	$D_7/D_5$ dB
700	-45.40	-39.44
1,000	-33.02	-33.20
1,500	-19.95	-26.13

Here we discuss the influence of the 7th intermodulation distortion power,  $D_7$ .  $D_7$  is given in Appendix (see (A.13)). Table 3 shows some numerical results of  $D_7/D_3$  dB and  $D_7/D_5$  dB for the parameters in Tables 1 and 2 at  $\Delta F$  of 700, 1,000, and 1,500 MHz. From the numerical results IM5 distortion power is dominant,  $D_7$  power is smaller than  $D_3$  and  $D_5$  by about  $-20$  dB and  $-26$  dB at  $\Delta F$  of 1,500 MHz. Since the influence of IM7 distortion power is negligibly small in this analysis, we focus on  $D_3$  and  $D_5$ .

#### 4. Numerical Results

We show some numerical results of CNDR. We define that  $D$  is the distortion power and is given by

$$D = D_3 + D_5.$$

Parameters used in the calculation are shown in Tables 1 and 2 (nonlinear LD). We assume the bandwidth,  $B$ , which is used in the PHS system for example.

First, we investigate the carrier power to IM3 distortion power ratio ( $CD_3R$ ), carrier power to IM5 distortion power ratio ( $CD_5R$ ), and CNDR versus  $\Delta F$  when the driving point of the OFD,  $T_1(f_c, \phi = 0)$  and  $T_2(f_c, \phi = 0)$  are

$$T_1(f_c, \phi = 0) = T_2(f_c, \phi = 0) = \frac{1}{2}.$$

Figure 6 shows  $CD_3R$ ,  $CD_5R$ , and CNDR versus  $\Delta F$  for carrier numbers of 3, 5, and 11. It is found from Fig. 6 that distortion power  $D$  becomes greater as the number of the carrier increases. The influence of IM5 distortion cannot be neglected at  $\Delta F = 4,500$  MHz, 2,000 MHz, and 1,000 MHz for 3, 5, and 11 carriers respectively in the case without control.

Next, we show CNDR in the case that the nonlinear compensation receiver shown in Fig. 5 is employed. Figures 7 and 8 show the plots for CNDR versus phase shift  $\phi$ . From Figs. 7 and 8, we find that the improvement of CNDR in controlling the phase shift,  $\phi = \phi_{min}$ , is better than  $\phi = \phi_{D3}$  and  $\phi = 0$  (without control).

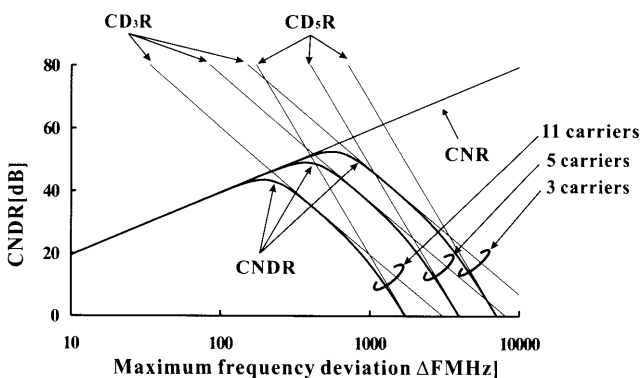


Fig. 6 CNDR versus  $\Delta F$  for the carrier numbers of 3, 5 and 11 carriers.

The phase shift control of  $\phi = \phi_{min}$  can obtain an improvement of approximately 0.7 dB in CNDR compared with the phase shift control of  $\phi = \phi_{D3}$  and 9 dB compared with the case without control for  $\Delta F = 2,000$  MHz and 3 carriers. For 11 carriers and  $\Delta F = 700$  MHz, an improvement of 2 dB in CNDR compared with  $\phi = \phi_{D3}$  and an improvement of 10 dB in CNDR compared with the case without control. Even if IM3 distortion power can be suppressed by controlling phase shift,  $\phi = \phi_{D3}$ , the IM5 distortion power can not be suppressed for large  $\Delta F$ . Consequently CNDR for  $\phi = \phi_{D3}$  is worse than CNDR for  $\phi = \phi_{min}$ . The phase shift control of  $\phi = \phi_{min}$  is effective. Next we examine the improvement of CNDR for various frequency deviations.

Figure 9 shows CNDR versus  $\Delta F$  for 3 carriers and 11 carriers. When comparing the improvement for  $\phi = \phi_{min}$ ,  $\phi = \phi_{D3}$  and the case without control in CNDR, we find that the phase shift control of  $\phi = \phi_{min}$  can get a wider maximum frequency deviation range for the phase shift control of  $\phi = \phi_{min}$  than the phase shift control of  $\phi = \phi_{D3}$  and  $\phi = 0$ . This is because the improvement in CNDR is effective for large

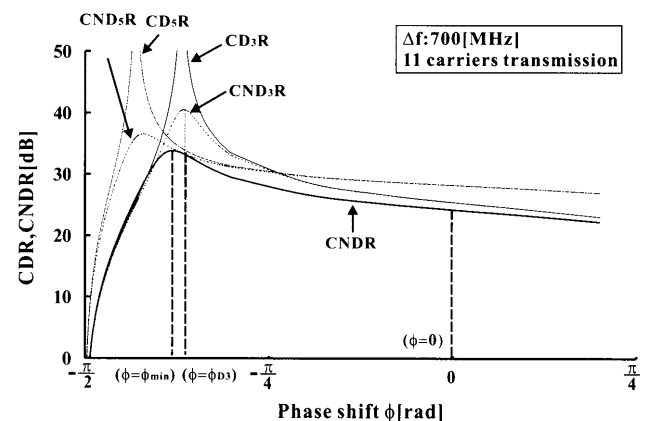


Fig. 7 CDR and CNDR versus phase shifter  $\phi$  at  $\Delta F = 700$  MHz for 11 carriers.

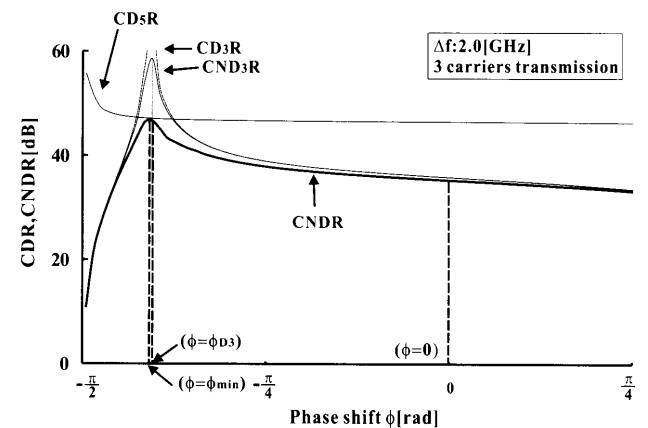


Fig. 8 CDR and CNDR versus phase shifter  $\phi$  at  $\Delta F = 2,000$  MHz for 3 carriers.

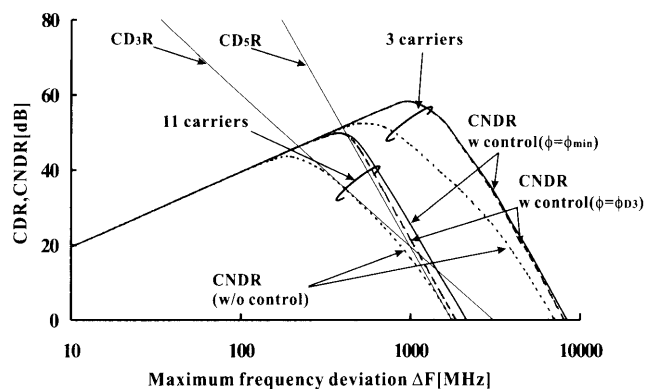


Fig. 9 CNDR versus  $\Delta F$  parallel among phase shift  $\phi_{min}$ ,  $\phi_{D3}$ , and the case without control (nonlinear LD).

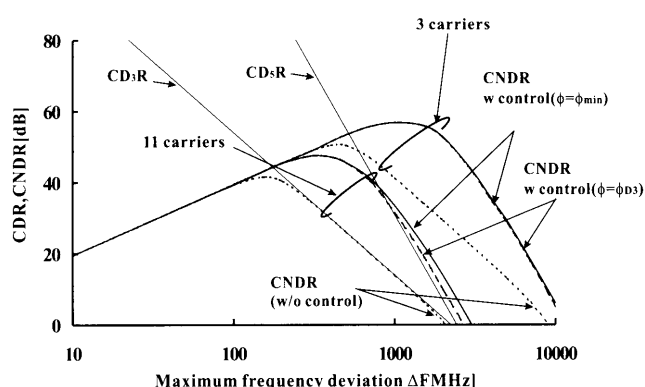


Fig. 10 CNDR versus  $\Delta F$  parallel among phase shift  $\phi_{min}$ ,  $\phi_{D3}$ , and the case without control (linear LD).

$\Delta F$ . It is found from Fig. 9 that the influence of IM5 distortion cannot be neglected when  $\Delta F$  is 1,000 MHz for 11 carriers. (A difference of approximately, 3 dB between the phase shift control of  $\phi = \phi_{min}$  and the phase shift control of  $\phi = \phi_{D3}$ .)

Figure 10 shows CNDR versus  $\Delta F$  in the case of employing a linear LD. The parameters of the linear LD are shown in Table 2. It is found from Fig. 10 that the CNDR for phase shift,  $\phi = \phi_{min}$ , is more improved than the CNDR for phase shift,  $\phi = \phi_{D3}$  and  $\phi = 0$  (without control) and a wider maximum frequency deviation range, as well as in the case of nonlinear LD.

By comparing CDR in a employing nonlinear LD with a linear LD, we observe that the maximum CDR of the nonlinear LD is larger than that of the linear LD. The maximum values are approximately 50 dB for 11 carriers in the case of the nonlinear LD and about 47 dB for 11 carriers in the case of the linear LD. This is because the nonlinear compensation can be obtained from the interaction between the nonlinearity of the LD and the MZI-type OFD shown in Figs. 3 and 4. On the other hand, in terms of the dynamic range, we find that the dynamic range of the linear LD is wider than that of the nonlinear LD. If a required CNDR is 30 dB, a maximum frequency deviation range, that is the dy-

namic range, of the linear LD is wider 200 MHz than that of the nonlinear LD for 11 carriers. We can find from these results that if a higher CNDR is required, it is more effective to employ a nonlinear LD than a linear LD, and if a wider dynamic range is required, a linear LD is more effective than a nonlinear LD.

## 5. Conclusions

In this paper, we have analysed IM3 and IM5 distortion power and calculated CNDR versus maximum frequency deviation  $\Delta F$  for the carrier numbers of 3, 5, and 11 carriers. From the results, it was found that the effect of intermodulation distortion power including IM5 was not negligible when the maximum frequency deviation  $\Delta F$  became large. Then we examined the effect of IM5 distortion versus  $\Delta F$  for 3 and 11 carriers. Accordingly the influence of IM5 distortion for 11 carrier is larger than that of IM5 distortion for 3 carriers. We showed that the designed nonlinear compensation technique was effective with consideration for intermodulation distortion including 5th order intermodulation distortion, and found that CNDR in the controlling phase shifter improved by approximately 2 dB compared with  $\phi = \phi_{D3}$  and improved by 10 dB compared with the case without control, for  $\Delta F = 700$  MHz and 11 carriers. It was found from comparison of a linear LD with a nonlinear LD that high CDR can be obtained to compensate for IM3 distortion, and a wide dynamic range can be obtained to compensate for IM5 and high-order intermodulation distortion. In this analysis, the improvements in CNDR and the dynamic range were about 4 dB and 200 MHz respectively.

## Acknowledgements

This paper is partially supported by the Grant-in-Aid for Scientific Research (B) No. 14350202, from the Japan Society for the Promotion of Science.

## References

- [1] S. Komaki, K. Tsukamoto, M. Okada, and H. Harada, "Proposal of radio highway networks for future multimedia personal wireless communications," ICPWC'94, pp.204-208, Bangalore, India, Aug. 1994.
- [2] D.C. Cox, "A radio system proposal for widespread low-power tetherless communications," IEEE Trans. Commun., vol.39, no.2, pp.324-335, Feb. 1991.
- [3] W.I. Way, R. Olshansky, and K. Sato, ed., "Application of RF and microwave subcarriers to optical fiber transmission in presence in recent and future broadband networks," IEEE J. Sel. Areas Commun., vol.8, no.7, pp.1230-1237, Sept. 1990.
- [4] S. Komaki, K. Tsukamoto, S. Hara, and N. Morinaga, "Proposal of fiber and radio extension link for future personal communications," Microwave Opt. Technol. Lett., vol.6, no.1, pp.55-60, Jan. 1993.
- [5] A.A.M. Saleh, "Fundamental limit on number of channels in subcarrier multiplex lightwave CATV system," Electron.

- Lett., vol.25, no.12, pp.776–777, 1989.
- [6] H. Al-Rawashidy and S. Komaki, Radio over Fiber Technologies for Mobile Communications Networks, Artech House Publishers, 2002.
- [7] R. Ohmoto and H. Ohtsuka, “Performance of FM double modulation for subcarrier optical transmission systems,” IEICE Trans. Commun., vol.E76-B, no.9, pp.1152–1158, Sept. 1993.
- [8] K. Kikushima, H. Yoshinaga, H. Nakamoto, C. Kishimoto, M. Kurobe, K. Suto, K. Kumozaki, and N. Shibata, “Optical super wide-band FM modulation scheme and its application to multi-channel AM video transmission systems,” IOOC’95, PD2-7, HongKong, 1995.
- [9] S.L. Woodward, “Lightwave CATV systems using frequency-modulated laser and interferometer,” Electron. Lett., vol.25, pp.1665–1666, 1989.
- [10] W.I. Way, Y.H. Lo, T.P. Lee, and C. Lin, “Direct detection of closely spaced optical FM-FDM Gb/s microwave PSK signals,” Technol. Lett., vol.3, pp.176–178, 1991.
- [11] G. Fiskman, R. Gross, J. Fan, and L. Kazovsky, “Performance optimization of directly modulated FM-SCM systems with optical discriminator,” Photon. Technol. Lett., vol.5, pp.845–848, 1993.
- [12] G. Yabre and J.L. Bihan, “Intensity modulation technique using a directly frequency modulated semiconductor laser and an interferometer,” J. Lightwave Technol., vol.13, pp.2093–2098, 1995.
- [13] G. Yabre, “Interferometric conversion of laser chirp to IM: Effect of the interferometer free spectral range on the output nonlinear distortion,” Photon. Technol. Lett., vol.8, pp.1388–1390, 1996.
- [14] K. Tsukamoto, S. Fujii, S.J. Park, and S. Komaki, “Theoretical consideration on nonlinear distortion suppression in directly optical FM microwave over fiber system,” Proc. Microwave Photonics 97, vol.FR3-2, pp.251–255, Sept. 1997.
- [15] S. Fujii, S.J. Park, K. Tsukamoto, and S. Komaki, “Proposal of nonlinear compensation scheme in optical direct FM fiber-optic microcellular communication system,” Proc. Optoelectronics and Communications Conference 98, vol.15A1-4, pp.312–313, July 1998.
- [16] K. Kumamoto, K. Tsukamoto, and S. Komaki, “Nonlinear distortion suppression scheme in optical direct FM radio-on-fiber system,” IEICE Trans. Commun., vol.E84-B, no.5, pp.1167–1172, May 2001.
- [17] G. Sato, Nonlinear compensation techniques for analog optical transmission systems, The Institute of Electronics, Information and Communication Engineers, pp.33–38, 1996.

## Appendix

We derive Eqs. (19), (20), and (23) in the following. At first Eqs. (7), (17), and (18) are substituted into (10) and (11) respectively, and we derive  $D_3$  and  $D_5$  as

$$D_3 = \frac{1}{2} \left( \frac{\pi}{FSR} r P_c \right)^2 \left[ \left( \gamma + \frac{m_k}{\Delta F} \alpha \beta - \frac{1}{6} \left( \frac{\pi}{FSR} \right)^2 \alpha^3 \right)^2 + \left( \frac{\pi}{FSR} \right)^2 \left( \alpha \beta + \frac{1}{2} \frac{m_k}{\Delta F} \alpha^3 \right)^2 \right] \times \left\langle (i_{in}^3(t))^2 \right\rangle_{f_n} \sin^2 \left( \frac{\pi f_c}{FSR} + \theta_3 + \phi \right) \quad (\text{A} \cdot 1)$$

$$D_5 = \frac{1}{2} (r P_c)^2 \left( \frac{\pi}{FSR} \right)^4 \left[ \left( \frac{\pi}{FSR} \right)^2 \left\{ \frac{\alpha^5}{120} \left( \frac{\pi}{FSR} \right)^2 \right. \right.$$

$$\left. - \frac{1}{2} (\alpha \beta^2 + \alpha^2 \gamma) - \frac{1}{2} \alpha^3 \beta \frac{m_k}{\Delta F} \right\}^2 + \left\{ \beta \gamma - \frac{1}{8} \left( \frac{\pi}{FSR} \right)^2 \alpha^3 \beta + \frac{1}{2} (2\gamma \alpha + \beta^2) \frac{\alpha}{\Delta F} m_k - \frac{1}{24} \left( \frac{\pi}{FSR} \right)^2 \frac{m_k}{\Delta F} \alpha^5 \right\}^2 \right] \left\langle (i_{in}^5(t))^2 \right\rangle_{f_n} \times \sin^2 \left( \frac{\pi f_c}{FSR} + \theta_5 + \phi \right), \quad (\text{A} \cdot 2)$$

where

$$\theta_3 = \tan^{-1} \left[ \frac{\frac{\pi}{FSR} (\alpha \beta + \frac{1}{2} \frac{m_k}{\Delta F} \alpha^3)}{\gamma + \frac{m_k}{\Delta F} \alpha \beta - \frac{1}{6} \left( \frac{\pi}{FSR} \right)^2 \alpha^3} \right] \quad (\text{A} \cdot 3)$$

$$\theta_5 = \tan^{-1} \left[ \left\{ \beta \gamma - \frac{1}{8} \left( \frac{\pi}{FSR} \right)^2 \alpha^3 \beta + \frac{1}{2} (2\gamma \alpha + \beta^2) \frac{\alpha m_k}{\Delta F} - \frac{1}{24} \left( \frac{\pi}{FSR} \right)^2 \frac{m_k}{\Delta F} \alpha^5 \right\} \div \left\{ \frac{\pi}{FSR} \left( \frac{\alpha^5}{120} \left( \frac{\pi}{FSR} \right)^2 - \frac{1}{2} (\alpha \beta^2 + \alpha^2 \gamma) - \frac{1}{2} \alpha^3 \beta \frac{m_k}{\Delta F} \right) \right\} \right]. \quad (\text{A} \cdot 4)$$

Therefore  $D_3$  becomes zero when

$$\sin^2 \left( \frac{\pi f_c}{FSR} + \theta_3 + \phi \right) = 0 \quad (\text{A} \cdot 5)$$

and  $D_5$  becomes zero when

$$\sin^2 \left( \frac{\pi f_c}{FSR} + \theta_5 + \phi \right) = 0, \quad (\text{A} \cdot 6)$$

so  $\phi_{D3}$  and  $\phi_{D5}$  are solved as Eqs. (19) and (20).

Next we derive Eq. (23).  $D_3$  and  $D_5$  are expressed as

$$D_3 = D_{IM3} \sin^2 \left( \frac{\pi f_c}{FSR} + \theta_3 + \phi \right) \quad (\text{A} \cdot 7)$$

$$D_5 = D_{IM5} \sin^2 \left( \frac{\pi f_c}{FSR} + \theta_5 + \phi \right), \quad (\text{A} \cdot 8)$$

where

$$D_{IM3} = \frac{1}{2} \left( \frac{A_3}{4} \frac{\pi}{FSR} r P_c \right)^2 \left( \frac{\Delta F}{\alpha} \right)^6 \left[ \left( \gamma + \frac{m_k}{\Delta F} \alpha \beta - \frac{1}{6} \left( \frac{\pi}{FSR} \right)^2 \alpha^3 \right)^2 + \left( \frac{\pi}{FSR} \right)^2 \left( \alpha \beta + \frac{\alpha^3 m_k}{2 \Delta F} \right)^2 \right] \quad (\text{A} \cdot 9)$$

$$D_{IM5} = \frac{1}{2} \left( \frac{A_5}{16} r P_c \right)^2 \left( \frac{\pi}{FSR} \right)^4 \left( \frac{\Delta F}{\alpha} \right)^{10} \left[ \left( \frac{\pi}{FSR} \right)^2 \left\{ \frac{\alpha^5}{120} \left( \frac{\pi}{FSR} \right)^2 - \frac{1}{2} (\alpha \beta^2 + \alpha^2 \gamma) - \frac{1}{2} \alpha^3 \beta \frac{m_k}{\Delta F} \right\}^2 + \left\{ \beta \gamma - \frac{1}{8} \left( \frac{\pi}{FSR} \right)^2 \alpha^3 \beta + \frac{1}{2} (2\gamma \alpha + \beta^2) \frac{\alpha m_k}{\Delta F} \right\}^2 \right]$$

$$-\frac{1}{24} \left( \frac{\pi}{FSR} \right)^2 \frac{m_k}{\Delta F} \alpha^5 \Big\}^2. \quad (\text{A} \cdot 10)$$

then

$$\begin{aligned} IMD(\phi) &= D_{IM3} \sin^2 \left( \frac{\pi f_c}{FSR} + \theta_3 + \phi \right) \\ &\quad + D_{IM5} \sin^2 \left( \frac{\pi f_c}{FSR} + \theta_5 + \phi \right) \\ &= \frac{1}{2} (D_{IM3} + D_{IM5}) - \frac{1}{2} \left\{ D_{IM3}^2 + D_{IM5}^2 \right. \\ &\quad \left. + 2D_{IM3}D_{IM5} \cos(2\theta_3 - 2\theta_5) \right\}^{1/2} \\ &\quad \times \cos(2\phi + 2\theta_{IMD}), \end{aligned} \quad (\text{A} \cdot 11)$$

where

$$2\theta_{IMD} = \frac{2\pi f_c}{FSR} + \tan^{-1} \frac{D_{IM3} \sin 2\theta_3 + D_{IM5} \sin 2\theta_5}{D_{IM3} \cos 2\theta_3 + D_{IM5} \cos 2\theta_5}.$$

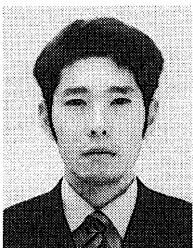
Consequently  $IMD(\phi)$  has the minimum value when

$$\cos(2\phi + 2\theta_{IMD}) = 1 \quad (\text{A} \cdot 12)$$

so  $\phi_{min}$  can be expressed as Eq. (23).

We substitute Eq. (1) into Eq. (8) and calculate the components of the IM7 distortion power,  $D_7$ , falling in  $n$ th frequency channel,  $f_n$ , of received RF signal is derived by

$$\begin{aligned} D_7 &= \left[ 2rP_c \left\{ (\alpha\gamma^2 + \beta^2\gamma) T_1^{(3)}(\phi) \right. \right. \\ &\quad + \frac{1}{4!} (12\alpha^2\beta\gamma + 4\alpha\beta^3) T_1^{(4)}(\phi) + \frac{10}{5!} \alpha^3\beta^2 T_1^{(5)}(\phi) \\ &\quad + \frac{6}{6!} \alpha^5\beta T_1^{(6)}(\phi) + \frac{\alpha^7}{7!} T_1^{(7)}(\phi) \\ &\quad + \frac{\alpha m_k}{\Delta F} \left( \frac{\gamma^2}{2!} T_1^{(2)}(\phi) + \frac{\beta^3}{3!} T_1^{(3)}(\phi) \right. \\ &\quad + \frac{1}{4!} (4\alpha^3\gamma + 6\alpha^2\beta^2) T_1^{(4)}(\phi) \\ &\quad \left. \left. + \frac{5\alpha^4\beta}{5!} T_1^{(5)}(\phi) + \frac{\alpha^6}{6!} T_1^{(6)}(\phi) \right) \right\}^2 \left\langle (i_{in}^7(t))^2 \right\rangle_{f_n} \end{aligned} \quad (\text{A} \cdot 13)$$

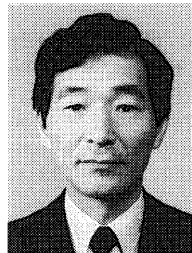


**Akihiko Murakoshi** was born in Hiroshima, Japan in March 14, 1979. He received his B.E. degrees in Communications Engineering from Osaka University, in 2002. He is currently pursuing his M.E. degree at Osaka University. He is engaging in research on radio and optical communication systems.



per Award of IEICE, Japan in 1996.

**Katsutoshi Tsukamoto** was born in Shiga, Japan in October 7, 1959. He received his B.E., M.E. and Ph.D. degrees in Communications Engineering from Osaka University, in 1982, 1984 and 1995, respectively. He is currently an Associate Professor in the Department of Communications Engineering at Osaka University, engaged in research on radio optical communication systems. He is a member of IEEE and ITE. He was awarded the Pa-



**Shozo Komaki** was born in Osaka, Japan in 1947. He received his B.E., M.E. and Ph.D. degrees in Communications Engineering from Osaka University, in 1970, 1972 and 1983, respectively. In 1972, he joined the NTT Radio Communication Labs., where he has engaged in repeater development for a 20-GHz digital radio system, 16-QAM and 256-QAM systems. From 1990, he moved to Osaka University, Faculty of Engineering, and engaging in research on radio and optical communication systems. He is currently a Professor in the Department of Communications Engineering at Osaka University. Dr. Komaki is a senior member of IEEE, and a member of the Institute of Television Engineering of Japan (ITE). He was awarded the Paper Award and the Achievement of IEICE, Japan in 1977 and 1994 respectively.